Int. J. Electrochem. Sci., 12 **(2017)** 733 – 746, doi: 10.20964/2017.01.55

International Journal of ELECTROCHEMICAL SCIENCE
www.electrochemsci.org

Short Communication

The Electrochemical Behavior and Heat Removal Study during the Solidification Process of an Al-base Alloy

O.R. Pérez[1,2], *O. Sotelo*[1], *M. Vázquez*[1,2], *S. Valdez*[1,*]

[1] Instituto de Ciencias Físicas-UNAM, Av. Universidad 1001, Col. Chamilpa, 062210, Cuernavaca, Morelos, México**.**
[2] Universidad Autónoma del Estado de Morelos-Research center in engineering and applied sciences, Av. Universidad 1001, Col. Chamilpa, 62210, Cuernavaca, Morelos, México.
[*]E-mail: svaldez@fis.unam.mx

Received: 25 October 2016 / *Accepted:* 19 November 2016 / *Published:* 12 December 2016

We study the effect that physicochemical phenomena attack the electrochemical degradation of ternary aluminum alloy. The chemical reaction on corrosion behavior has been correlated with extraction of heat during the solidification process. The scope of the present work is the analysis of the evolution of chemical degradation into aluminum alloys by the influence of the imposing high cooling rate during liquid to solid formation. Within the framework of a thermodynamic phenomenon, the cooling rate has been estimated as the single most important influence on the microstructural behavior. The first approach involves the effects of dendrite arm size and the solute distribution for the ternary aluminum alloy. In fact, the extreme rates of heat removal have been correlated with a good corrosion resistance for the aluminum alloy, which has been linked with the appropriate composition and refined microstructural features. Moreover, the evolution of the growth rate of the solid, which occurs during the casting, might lead both to their mechanical properties, and chemical degradation. Several metallic systems have been considered for use as approach to explain of such chemical mechanism to corrosion degradation. The effect of electrochemical parameters such as E_{corr} and I_{corr} values has been deduced, and will also be discussed the initial corrosion kinetics and the corrosion resistance behavior.

Keywords: Electrochemical degradation, Electrochemical Impedance Spectroscopy, Bode phase diagram, aluminum base alloys, cooling rate, solidification process.

1. INTRODUCTION

Electrochemical degradation occurs when the metallic surface is in contact with anions and cations in a solution substance [1]. The challenge to the process in aluminum alloys is the metal oxide or hydroxide formed after the corrosion affected by physicochemical conditions [2]. The surfaces

protected should be taken over the exclusive protection. However, the surface inhomogeneties, such as donor states of passive films influence the corrosion processes [3, 4].

Aspects of processing, microstructures, kinetics, and interfacial reactions affected the passive film, which may be central to study the corrosion resistant aluminum alloys. Innovative approaches undertaken by many researchers [5, 6] have studied the oxide formation of metals [6], which they have described initially with the chemisorbed oxygen molecule [7, 8]. To achieve consistent electrochemical analysis from aluminum alloy the oxide passivating layer over the metal surface should be considered as a key factor.

The literature regarding as a possible candidate for ternary aluminum alloys its degradation by the oxygen molecule dissociations over the metal surfaces, which have higher gauge factors to attract the aluminum surface [9, 10]. In our approach, the oxide passivating layer has been considered one reason that influences the corrosion degradation mechanism. This point is illustrated with a comprehensive review [10] of the combination with performance characteristics correlated with their synthesis, and the fundamental physical phenomena involved during the solid to liquid process involved.

Furthermore, microstructure studies indicate that is an important characteristic associated with the presence of thermodynamic properties of the material synthesis on electrochemical degradation [11, 12]. In a recent study [13, 14], has been also considered the influence of gas entrapment, solidification shrinkage, hydrogen dissolution, and interstitial porosity as a result of the considerable important factor of mechanism degradation in saline media. In fact, it has been shown that the mechanism degradation is consistent with the detrimental of microstructural phases combined with precipitates plus eutectic phases that can occur sequentially and simultaneously. The underlying reason for this electrochemical behavior is most likely that, high-performance and processing technique emphasis the composition, processing, and microstructure relationship.

Performance improvements for structural materials include attractive combinations of composition, microstructures, processing, and properties achievable through the manufacturing process. In fact, successful at property - microstructure has been critically correlated with parameters of the synthesis and manufacturing process [8, 15, 16]. According to the highly attractive combinations of microstructure and mechanical properties achievable through rapid solidification technology we have been synthetized the alloy with a rapid extraction of thermal energy as a means of improving the behavior of existing alloy systems. The rapid extraction of heat can give raise the most important influence on the microstructural refinement due to the imposing high cooling rate occurs before, during and after the transition from the liquid state to solid alloy.

The extreme rates of heat removal promote the formation of unique microstructures, as well as unusual structures, qusicrystalline phases, size refinement or metastable phases [17, 18, 19]. Furthermore, other characteristics could be frequently associated with the rapid solidification process. This relation is few recurrently given with the electrochemical degradation, which is still in development, many of the alloys systems studied could be now exploit their excellent microstructural properties with the electrochemical behavior in applications not originally envisioned.

The electrochemical degradation describes, in general terms, the reaction of a surface material with its surroundings environment. This process also involves property relationships with chemical

nature of alloying, alloy composition, the internal structure arrangement as determined by casting conditions as well as thermomechanical processing [20, 21]. This article describes the nature and chemical alloy composition associated with their electrochemical performance processing by conventional casting with advantage of high cooling rate during the solidification phenomena. In the literature, make it imperative to explain the combination of electrochemical properties and control of heat removal, with all this in mind, this paper provide a contribution to advance in the field of electrochemical degradation intentionally assigned with a potential light/weight alloy manufactured by conventional casting taking advantage on the mould design in order to get a fast cooling rate.

2. EXPERIMENTAL PROCEDURE

2.1 Synthesis with high cooling rate

A family of high-performance ternary aluminum with magnesium plus silicon alloy has been developed that provides a relatively high strength to weight ratio with a good resistance to certain types of corrosion degradation [22, 23]. The stoichiometric composition of the experimental aluminum base alloy was $Al_{96.3}Mg_{1.7}Si_{1.5}Fe_{0.5}$; this chemical formulation is substantially higher iron content in order to control microstructure phases. For convenience, the alloy was denoted as AlMe.

The simple an inexpensive as-casting process was used to prepare an ingot AlMe alloy by using a resistance electrical furnace, previously preheated at 300°C during ten minutes. Melting aluminum and magnesium with a melting point of 650ºC and 660ºC respectively were cutting in ingot small pieces with 99.90% purity.

The chemical alloy elements were put into an alumina crucible using molten mixture of potassium and sodium chloride salts at 680ºC with the shielding argon gas to inhibit the contact with the environmental and prevent oxidation losses. The liquid AlMe has been overheated 150ºC during the preheated silicon addition, which was done via refractory feeder tip directly into the alumina crucible. The melt-bath was homogenized by intense mechanical stirring at 1150rpm for fifteen minutes to have a uniform distribution of silicon particularly and then was poured into a wedge-shaped liquid nitrogen-cooled copper mould. As a high thermal conductivity, copper mould design has been selected for heat exchanger, which possesses the ability to accelerated cooling, in this case, by conducting and transfer thermal heat efficiently.

In order to measure, in situ, the cooling rate at there different cooling zones during the solidification phenomena, thermocouple temperature sensors Chromel-Alumel K-type wire were used.

The thermocouple wires were insulated in a ceramic fiber and were introduced centrally from the top of the mould cavity where the temperature or temperature gradient could be measured. To illustrate the effects of changes in cooling rate from the same wedge ingot, the cooling curves have been recorded from time and temperature dates compiled from specific distances along the wedge mould during the transformation to liquid melting into a solid AlMe ingot. The corresponding cooling rate values showed cooling rate variations from the three solidification regions throughout the same ingot.

2.2 Samples preparation

Expectations that the effect of cooling rates influences the mechanical properties have been taking account. In addition, the electrochemical degradation performance in relationship with the cooling rate effect has also been assumed during the samples surface research. Specimen surfaces for mechanical properties were prepared to get an accurate result the test surface does not digress more than 2°, considering specifically Vickers indents we follow the standard technique of grinding with SiC up to 1000 grade emery papers and mechanical polishing with Al_2O_3 water suspension solution.

To minimize damage from surface samples, the working electrode surfaces from AlMe alloy were degreased in acetone; washed thoroughly in double distilled water and kept in a desiccator prior to immersion and Potentiodynamic polarization tests. A saline solution, 3.5 % NaCl, prepared from analytical grade reagents with deionized water. As a working electrode, both walls of the AlMe samples were covering with enamel, except for $1cm^2$, which was the surface, exposed to the solution and then the Electrodes were connecting a wire to one side of the sample

2.3 Measurement of Micro-Vickers hardness

Vickers hardness is a critical test associated with a general indication of the strength of the metallic material. The Vickers measurement has been suitable for a wide range of hardness material and of its resistance to scratching and to wear [24].

In addition, to appearing in this mechanical behavior the quality of firmness created by cohesion of chemical elements composing a material, as evidence by resistance to penetration, abrasion, scratching, cutting or shaping [25]. In particular, careful process has been carried out for the AlMe samples with different cooling rate during the solidification process. Strategy has been centered on correlate the surface resistance to penetration in the field of cooling rate processing. Additional effort has been need to driving force between the resistance to permanent indentation and the electrochemical behavior. Vickers hardness (VHN) was measured using a Shimadzu microhardness testing machine with 980-mN load and a 15-s loading time on the cross-sections of the metallic samples.

2.4 Potentiodynamic polarization

In order to describe the reaction of the AlMe alloy with its surroundings the corrosion resistance property has been studied by electrochemical testing. According to the manufacture processing, the electrochemical behavior could be related with parameter of synthesis. The process also has effect on atomic arrangement, mechanical properties, and the changes or damage of an electrochemical nature. Potentiodynamic polarization test has been done with a Gamry PCI4/300 potentiostat as electrochemical analyzer and DC105 software was used for collecting the current density expressed in $\mu A/cm^2$ and potential E_{corr} [V] as data acquisition. In this research, potential corrosion (E_{corr}), corrosion rate expressed in mm/year (also named corrosion velocity, V_{corr}), and corrosion current density (I_{corr}) values were estimated by the Tafel extrapolation method. This

considers each electrochemical reaction as the logarithm of the current density varies linearly with the electrode potential. The potentiodynamic current-potential curves were recorded by changing the working electrode potential from -700mv to +700mV at open-circuit potential (OCP), E_{corr}, with 1 mVs^{-1} scan rate at 22 ℃. The experimental procedure from the Potentiodynamic test were carried out using a standard three electrode configuration: saturated calomel as a reference with a platinum electrode as counter also known as auxiliary electrode, and the sample as the working electrode in where the potential difference between the working electrode and the Reference Electrode is well defined. The electrolyte contained in the standard cell was an aerated electrolyte solution with NaCl reagent grade at 3.5% diluted in deionized water. All the potentials refer to the calomel electrode. The potential sweep rate was 10 mV/min at 22 ℃.

2.5 Electrochemical Impedance Spectroscopy

The study of the impedance associated with the frequency of amplitude AC perturbation has been conducted using a Gamry PCI4/300 potentiostat. In addition, has been used a Gamry EIS300 software for recording of impedance spectra, which is a data representation of input and output signals. The overall process has been distinguished as a non-destructive procedure, and also as an electrode process where the interface provides information about its structure and reactions taking place in the studied material.

The Electrochemical Impedance Spectroscopy (EIS) experimental measurement provides data to analysis by coupling the AlMe working electrode into a glass corrosion cell that contained the aqueous electrolyte solution, a platinum counter electrode and a saturated calomel reference electrode (SCE). In order to analyze the system response to the application of a periodic small amplitude AC signal, and because of its value engineering opportunities, the EIS process has been developed with AC amplitude small enough of 10 mV AC signal, plus it was used a frequency (Hz) range of 100 mHz to 100 kHz. The electrode process has been described using an equivalent circuit as shape of Bode plots, allow us to describe the time dependent quantitative information about the reactions occurred of electrode-solution interface.

3. RESULTS AND DISCUSSION

A key element on this research lies on the process materials plus their effect on the electrochemical behavior associated with the effect of the cooling rate. Even though few studies have been reported [3, 5, 25] earlier on the effect of cooling rate on the surface degradation and electrochemical behavior of AlMe alloy. In this study, the correlation between electrochemical associated with mechanical properties has been studied with the Potentiodynamic polarization results and Vickers response principally.

The electrochemical degradation of cast aluminum alloys shows various reactions between the surface alloy and its environmental surroundings. The chemical reactions and physicochemical process

occurs sequentially during the electrochemical corrosion of the aluminum alloys. The electrochemical process involves the interaction of electrons from the surface of AlMe with the oxygen in order to the alloy back into their native oxide forms. The chemical reactions of AlMe alloy has been considered that occurs at the solid/environment interface, which can be broken down into anodic metal dissolution and the conforming cathodic reactions of hydrogen evolution and oxygen reduction [26, 27].

Reaction of aluminum anodic processes.

$2Al + 3O^{-2} \rightarrow Al_2O_3 + 6e^-$

$Al \rightarrow Al^{+3} + 3e^-$

The corrosion process initiate with the presence of the oxygen on the metallic surface, however the structure and composition of metallic phases and/or inclusions could affect the corrosion process and the initial reactions. Others factors that could affect the degradation in the corrosion process involves the composition of the electrolyte and the physical changes in their environmental. For the case of an anodic surface depletes electrons from the metallic alloy, such reactions could be

$H_2O + e^- \rightarrow H\ (adsorbed) + OH^-$

$H_2O \rightarrow OH + H^+ + e^-$

$H_2O \rightarrow O + 2H^+ + 2e^-$

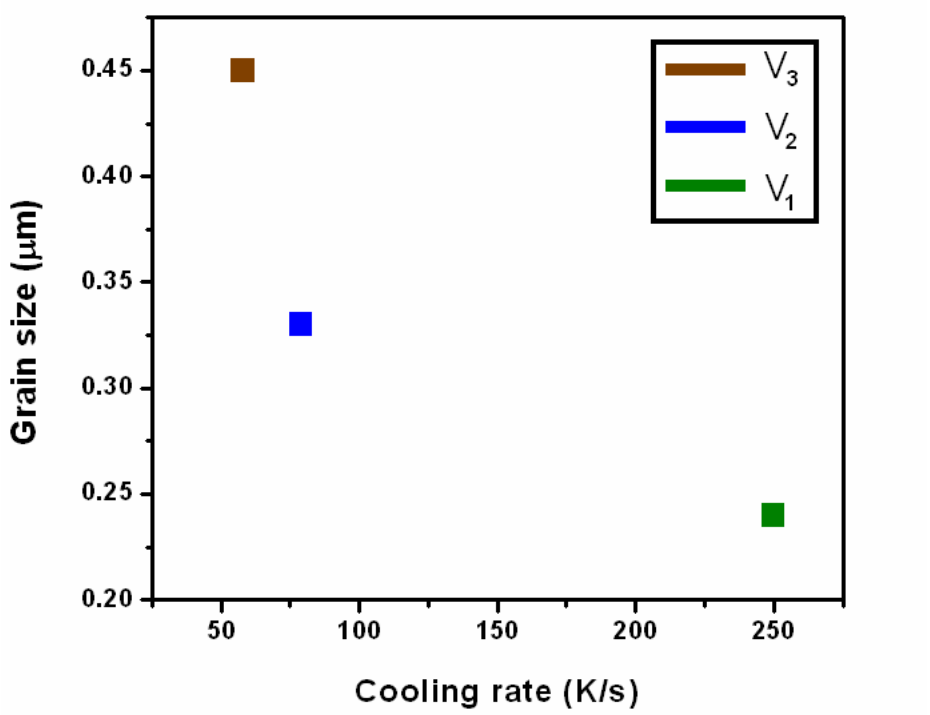

Figure 1. Relationship between cooling rate plus grain size for AlMe alloys. In the electrochemical degradation, the metallic alloy acts as a conductor of electric current I flowing through metallic surface plus electrolyte, in where metallic surface has been influenced by the grain boundary.

Specifications for the electrochemical reactions involve a complete understand about the dissolution events. Several measurements have been taken especially for light metallic alloys involving magnesium, aluminum and several electrolytes. To improve the understanding of the reactions

involving for a fast solidification process, the aim of the present work is determine the role of the cooling rate associated to the general electrochemical degradation and correlated with their mechanical properties.

According all this in mind, we focus on determine the cooling rate values, which were reached by using the copper mould. In either case, the resistivity of copper is 77 K and has a low cost. Emphasis on the high cooling rates; the copper mould was cooled by liquid nitrogen with the advantages of easy to manufacturing and simplicity mould design. On the other hand, the copper can produce high cooling rates for a conventional as-cast [4, 13], that is historically the conventional process for a metallic alloy route. Currently, the AlMe alloy has been solidified at three different cooling rates of 58, 79 and 250 K/s grown during liquid nitrogen-cooling conditions into copper wedge mould. The cooling rate increase when the mass of alloy between the two walls of copper is fewer.

The difference in the cooling rate values has been related with the wedge copper design. The wedge-shaped copper mold, 50-mm wide, was tapering from 15 mm to its tip over a distance of 200 mm. These cooling rate data demonstrate that it is possible to generate a rapid solidification through a high cooling rate controlled by the copper mould. In this figure we observed three different values of cooling rate from the same metallic alloy sample. In figure 1, we denote the V_1 as the region with the copper walls very close together. The V_2 position has been associated with the middle region of the copper mould. Finally, the V_3 point corresponds to the topper zone of the wedge copper mold.

Regarding the process of heat transfer in the mold from the liquid AlMe alloy, several mechanisms has been commonly considered, such as the conduction inside the bath liquid AlMe alloy [27], other approaches should be the convection, conduction and radiative heat transfer across the mould wall; other important factors include conduction through the mould, which should be considered simultaneously with convective heat transfer from the mould to the environment, this approach combined the geometry of copper mould [28, 29]. The practical implication derived from this kind of solidification process has an extensive evaluation with the phases and microstructure, which is a condition to introduce in this research just exclusively the grain size. It was further determined that the cooling rate is strongly associated with grain growth, texture, and size. This AlMe alloy takes advantage of the fact that the aluminum base of the alloy has been exhaustive studied, while the correlation between cooling rate and grain size is a useful step that indicates an appropriate level of grain boundaries describing the relationship with the electrochemical degradation. In an attempt to obtain that correlation, the measurement of grain size revealed a refinement at high cooling rate, as can be seen in Figure 1. As demonstrated in Figure 1, the grain size measurements plotted against the cooling rate values. We can observe that cooling rate has a very significant effect on the grain size of AlMe alloys. The properties usually advantageous in refinement grain size are either of little relevance or disadvantageous in grain boundaries as a hypothesis for the possibility to increase the electrochemical degradation by intergranular corrosion cracking. In the case of high cooling rate named (V_1 = 250 K/s), the influence of this parameter plays a critical role in the final grain size (0.45μm). This refinement is attributed to the presence of high number of nucleation sites growing at the same time and by increasing the grown rate, which is defined by the next equation [14, 30].

$$Zs = 1.1\ \left(\dot{N}/G\right)^{0.5}$$

Where $\dot{N}$ is the nucleation rate; G is the grain growth and the refinement is expressed by the Z. The grain growth behavior has been discussing has primarily been related to what has happened in the electrochemical behavior and their correlation with microhardness as an important mechanical property. In fact, the mechanical properties of polycrystalline alloys depend critically on the average grain size. Instead, therefore, attempts were made to improve the resistance to reduce the danger of alloys surface by environmental degradation. With respect to cooling rate during solidification that has been considered as the single most important influence on the grain refinement, this conception has been reflected in the figure 1 where has been observed that the rate of cooling is a key variable in the grain size. The concept of cooling rate should has affect the resultant of microvickers hardness, which is also interesting to note that when grain boundaries constitute a large fraction the strength of alloys increase by the difficulty in the dislocations motion [31].

Table 1 compares the mechanical characteristics of the AlMe alloy, one of the primary concerns with this type of results, has been improve of mechanical properties. In this table 1, the yield tension stress (YTS), and microhardness Vickers has been increased when the cooling rate increase from 58 to 250 K/s. Microhardness is a commonly used property usually defined as resistance to permanent indentation; since their developed in 1922 uses a pyramid-shaped diamond indenter in our days have been developed in atomic force microscopes and nanoindenters, to estimate hardness at penetration depths as low as 20 nm. However, what we have been showed in table 1 has primary been related with the effects of high cooling rate, which improves the solute distribution in both microstructures, regions along matrix and grain boundaries. Some of these results are agreed with previous research [6, 31], in which has been contributed to hardening of the solid solution as an example, the refinement has been associated with an extensive distribution of silicon particles in the interdendritic regions which stress resisting dislocation motion. It has been few reported experimentally in nanosize metallic alloys that the higher strength could be related with less resistant to corrosion because the alloying additions plus a grain refinement facilities the electrochemical degradation process [32].

Table 1. Mechanical parameters related with the AlMe alloys associated with the different cooling rate have been obtained by conventional casting. The electrochemical process should be influenced by the cooling rate due to the presence of phases formed during the casting.

Cooling rate	Mechanical Properties		
(K/s)	Vickers (MPa)	YTS (MPa)	UTS (MPa)
$V_1 = 250$	115	155	281
$V_2 = 79$	99	143	270
$V_3 = 58$	91	135	262

Since mechanical properties such as strength and hardness have been mainly depended on its microstructure, the objective of different research has been devoted to refining the grains of the alloys, in order to improve the mechanical properties [5, 32, 33]. In general, the electrochemical behavior of

solute and solvent plus the alloy microstructure have been influenced by solidification conditions such as the cooling rate. A direct connection of electrochemical behavior appears in literature with the alloy composition and manufacturing process on the metallic material performance, which improves mechanical properties and corrosion resistance.

The corrosion or electrochemical degradation deals with several chemical reactions and material transport that can supply or remove some microstructural phases. Electrochemical process, however, can be considered as irreversible processes in which the attainment of equilibrium involves more than a few chemical reactions. The knowledge and applications of a chemical reaction allows reporting the formation of chemical products described by chemical equations. For the reason that so various reactions should appears in the electrochemical degradation, the equilibrium constant of the chemical reaction help us to predict the chemical reactants and products that will happen.

A preliminary list of balanced chemical equations plan to make the most chemical products formed if or when the reactants and products have been consumed during the electrochemical process when the reaction is initiated. It can be seen from Table 2 the list of chemical equations associated at the appreciable reactions related with the most abundant chemical elements from the AlMe alloy.

Table 2. The different chemical reactions from oxidation process occurring for the AlMe alloy expressed in chemical equations for the electrochemical process and their standard reduction potentials.

Standard reduction Potentials E^o volts (Aquous solution, 25º)	Chemical equation and Half reaction
-0.147	$Si_{(s)} + 4H^+ + 4e^- \rightarrow SiH_{4\,(g)}$
-0.990	$SiO_{2\,(s)} + 4H^+ + 4e^- \rightarrow Si_{(s)} + 2H_2O$
-2.328	$Al(OH)_4 + 3e^- \rightarrow Al_{(s)} + 4OH^-$
-1.66	$Al^{3+} + 3e^- \rightarrow Al_{(s)}$
-2.690	$Mg(OH)_{2\,(s)} + 2e^- \rightarrow Mg_{(s)} + 2OH^-$
-2.37	$Mg^{2+} + 2e^- \rightarrow Mg_{(s)}$
0.000	$2H^+ + 2e^- \rightarrow 2H_{2\,(g)}$
-0.828	$H_2O + e^- \rightarrow 0.5\,H_{2\,(g)} + OH^-$
2.560	$OH + H^+ + e^- \rightarrow H_2O$
2.430	$O_{(g)} + 2H^+ + 2e^- \rightarrow H_2O$
1.229	$0.5\,O_{2\,(g)} + 2H^+ + e^- \rightarrow H_2O$

Modernization and improvement computer programs or computer simulations have been generally accepted that cathodic polarizations represent the oxygen reduction and hydrogen evolution reactions in aerated saline media [34, 35, 36]. The redox chemical reaction of the first oxidation function include the corresponding anodic and cathodic half reactions, these oxidations equations has been correlated with the oxidation potential. In which, temperature influence the standard potential, E^o (T) and correlated with the equilibrium constant, K [37, 38].

$$E^o\,(T) = E^o + \left(\frac{dE^o}{dT}\right)\Delta T$$

$$K = 10^{\frac{nFE^o}{RTIn10}}$$

It can be seen that all species are aqueous, *n* is the number of electrons in each half-reaction, *F* is the Faraday constant, and *R* is the gas constant.

As we pointed out in this paper, the role of the cooling rate associate to the general corrosion reactions means to improve surface corrosion resistance. The degree, or extents, of oxidation environment provide a relative influence, which is widely related with temperature, concentration and the type of elemental chemical aggressive. It is often useful to indicate the electrochemical measurements with respect to the potentiodynamic polarization test, and from the viewpoint of the electrochemical degradation the electrochemical impedance was conducted. Currently, the difference in the electrochemical behaviors of AlMe alloy has been showed in figure 2. It represents the structural damages that accompany the surface degradation at different cooling rate by the potentiodynamic polarization curve. Figure 2, also shows that the three AlMe samples with different cooling rate display an active corrosion behavior. In addition, the corrosion current density i_{corr} decrease, and leads to shifting of the corrosion potential E_{corr} towards the positive side.

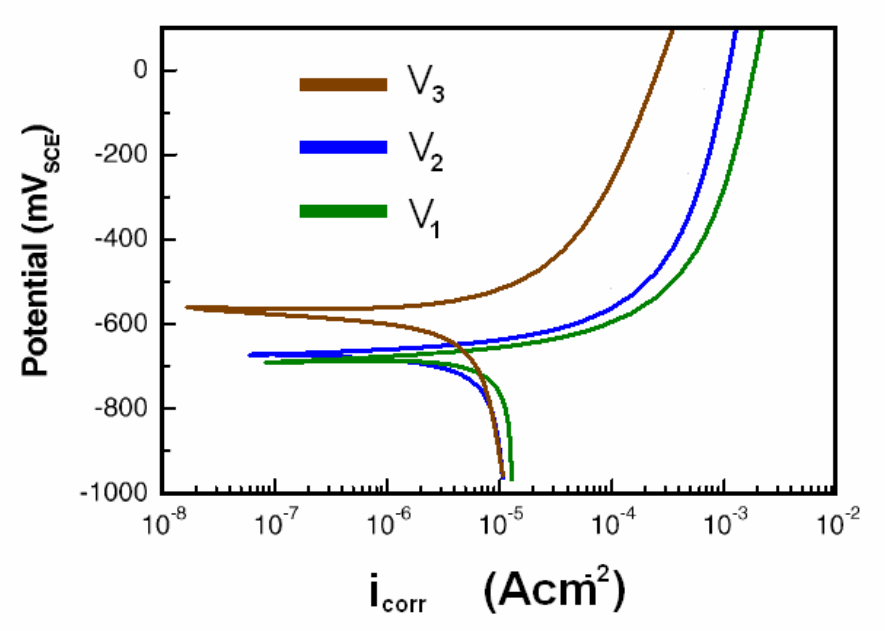

Figure 2. Potentiodynamic polarization curve of AlMe alloy at different cooling rate (K/s) expressed by V_1, V_2, and V_3 with cooling rate values of 250, 79, and, 58 respectively.

The polarization curves exhibit linear Tafel behavior in the *E* Vs *log (i)* plots, in which the intersection point corresponds to corrosion current density (i_{corr}) or corrosion rate. The equilibrium of the corrosion process related with the electrochemical potential of the AlMe has been estimated by the current density i_{corr}, in the Stearn-Geary equations [39, 40] as shown in equation (2):

$$B = \frac{\beta_\alpha \beta_\chi}{2.303\left(\beta_\alpha + \beta_\chi\right)} \quad (1)$$

$$R_p = \frac{B}{i_{corr}} = \frac{\left(\Delta E\right)}{\left(\Delta i\right)_{\Delta E \to 0}} \quad (2)$$

The *B* constant is determined using both cathodic and anodic reactions by anodic and cathodic Tafel slopes β_α and β_χ from the curve branches in volts/decade by Eq. (1). Within a few millivolts of the corrosion potential *Rp* links to the ratio between the potential shift ΔE and the equivalent current change Δi in a polarization test.

For instance, the figure 2 suggests that increase of high cooling rate hindered the electrochemical attack, which prevents the dissolution of the AlMe alloy. Another important factor examining the electrochemical degradation is the addition of a less noble chemical element such as magnesium (Mg), as a first approximation it may be assumed that magnesium did not lower the corrosion resistance. From this results could be related with a better solute homogenization and minor presence of secondary phases due to the cooling rate is higher. While, not a particularly picture of the oxide passivating layer is often the first line of defense against the corrosion.

Table 2 summarizes data from plots appearing in potentiodynamic polarization curve of AlMe alloy in relationship with the heat removal from the solidification route. It has been few studied the relationship that compared conventional solidification, chemical nature and composition of the AlMe alloy with their corrosion behavior. By contrast, there have been many studies that show the corrosion resistance of aluminium and its alloys; therefore, further study is needed for the electrochemical degradation in alloys rapidly solidified as the case of AlMe alloy in this work. This is the reason that high cooling rate associated with the heat transfer in bulk alloys rapidly solidified has been attracted increasing our attention from the view of electrochemical degradation in several electrolytic media as potential future research.

Table 2. Electrochemical parameters associated with high cooling rate, medium cooling rate and low cooling rate while heat removal occurs during the solidification process.

Solidification parameter	Electrochemical parameters	
Cooling rate (K/s)	Corrosion potential (E_{corr}) (mV)	Current density (i_{corr}) (μAcm^{-2})
V_1 = 250	-691	1.28
V_2 = 79	-674	1.52
V_3 = 58	-560	3.69

Overall, after taking account the analysis of the impedance which measure of the ability of a circuit to resist the flow of electrical current, their response has been expressed by Bode phase in figure 3. The graph representation exhibits log frequency against the phase-shift and both the absolute values of the impedance ($|Z|=Z_0$).

Bode phase on figure 3 shows current density and corrosion potential is possible to observe that AlMe alloy with high cooling rates is an improved material with better corrosion resistance, which increased for high cooling rates and provide enhanced electrochemical corrosion behavior.

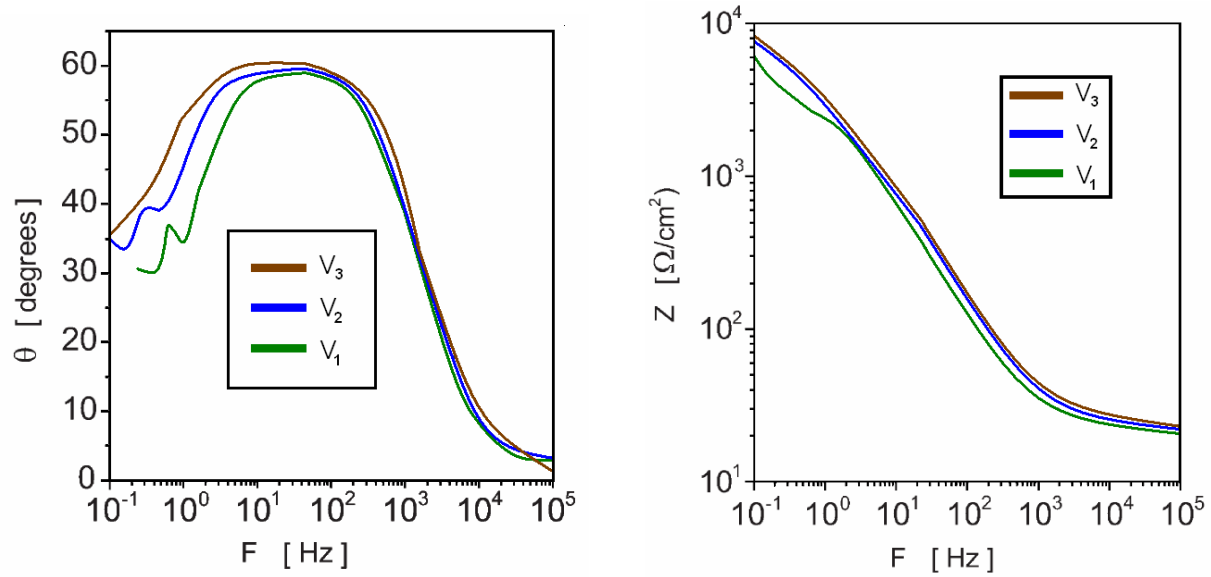

Figure 3. Electrochemical impedance spectroscopy of Bode phase for the AlMe alloy at three different cooling rate.

Electrochemical corrosion resistance of AlMe alloy in as-cast condition could be related with the aluminum alloys capacity to form passive films. The protector layer is formed by the diffusion of Al atoms through the grain boundaries to the surface of the alloy and to form the protective passive layer. The relationship between cooling rate with mechanical and electrochemical properties of the AlMe alloy, could be explained by the grain refinement.

The improve of corrosion resistance of the AlMe alloy with high cooling rates might be attributed to the solute entrapment during the solidification when is cooled at high rates, due to the presence of secondary phases does not occurred holding an Al matrix principally. Similar conclusions were drawn by a research that studied the influence on AM50 alloy [37, 38, 41].

4. CONCLUSION

The following conclusions could be obtained from the electrochemical results combined with mechanical properties and grain refinement of AlMe alloy:

- Electrochemical test results have shown that high cooling rate present the higher corrosion resistances than low cooling rate, due to grain refinement, the homogeneous solute distribution, and probability by Al alloys capacity to form passive films.
- High cooling rate can be obtained from the wedge mould shape cooled by liquid nitrogen; the highest cooling rate obtained has been 250 K/s.
- A grain refinement was generated when the cooling rate increases.
- Mechanical properties especially yield tension stress, ultimate tension stress, and microhardness Vickers were improve for high cooling rate. These results are associated with the grain refinement.

ACKNOWLEDGEMENTS
The authors gratefully acknowledge the observations and prompt response to Dr. Valdez. The present project has been supported by DGAPA-UNAM program Award No. PAPIIT-IT101112 and for funding the research project CONACyT #178563.

References

1. Lin, G.S. Frankel, W.H. Abbott, *J. Electrochem. Soc.*, 160 (2013) C345.
2. H.X. Liu, Y. Hu, X. Wang, Z.B. Shen, P. Li, C.X. Gu, H. Liu, D.Z. Du, C. Guo, *Mater. Sci. Eng*. A564 (2013) 13.
3. K. Jüttner, *Electrochim. Acta*, 35 (10) (1990) 1501.
4. M.I. Pech-Canul, A. Bautista-Hernández, M. Salazar-Villanueva, S. Valdez, *Mater. Design*., 44 (2013) 325.
5. I.G. Katz, R. Kosloff, and Y. Zeiri, *J. Chem. Phys*., 120 (2012) 19.
6. I. Martínez, C. Andrade, *Corros. Sci.*, 50 (10) (2008) 2948.
7. Z.Y. Zhang, H. Zhao, H.Z. Zhang, Z.S. Yu, J. Hu, L. He, J. Li, *Corros. Sci*., 93 (2015) 120.
8. Chen Pan, Li Liu, Ying Li and Fuhui Wang. *Corros Sci.*, 73 (2013) 32.
9. Lim, Tae Seop, Hyun Sam Ryu, and Seong-Hyeon Hong. *Corros. Sci.*, 62 (2012) 104.
10. Y. Wang, J. Wang, J. Zhang, Z. Zhang. *Mater. Corros*., 56 (2) (2005) 88.
11. R.F. Zhang, G.Y. Xiong, C.Y. Hu. *Curr. Appl. Phys*., 10 (2010) 255.
12. L. Wang, L. Chen, Z. Yan, H. Wang, J. Peng, *J. Alloys Compd*., 480 (2009) 469.
13. S.K. Bhambri, *J. of Mater. Sci*., 21 (1986) 1741.
14. Ç. Fatih and S. Kurnaz. *Mater. Desig.*, 25 (2005) 479.
15. W.R. Osório, J.E. Spinelli, N. Cheung, A. Garcia, *Mater. Sci. Eng., A*420 (2006) 179.
16. A.D. Mazzoni, M.A. Sainz, A. Caballero, E.F. Aglietti, *Mater. Chem. Phys.*, 78 (1) (2003) 30.
17. R. Arrabal, E. Matykina, T. Hashimoto, P. Skeldon, G.E. Thompson, *Surf Coat Technol.*, 203 (16) (2009) 2207.
18. J. Ding, W. Yuan, J. Li, H. Zhu, C. Deng, F. Dalard, *Adv. Mater. Res.*, 399–401 (2012) 851.
19. J.E. Spinelli, M.D. Peres, and A. Garcia, *J. Alloys Compd.*, 403 (2005) 228.
20. N. Godja, N. Kiss, C. Löker, A. Schindel, A. Gavrilovic, J. Wosik, *et al., Tribol. Int.*, 43 (7) (2010) 1253.
21. L. Wang, L. Chen, Z. Yan, H. Wang, J. Peng, *J. Alloys Compd*., 480 (2009) 469.
22. J. Liang, P. Bala Srinivasan, C. Blawert, W. Dietzel, *Electrochim. Acta.*, 55 (2010) 6802.
23. H.S. Ryu, S.J. Mun, T.S. Lim, H.C. Kim, K.S. Shin, S.H. Hong, *J. Electrochem. Soc*., 158 (2011) C266.
24. P.D. Bilmes, C.L. Llorente, C.M. Méndez, C.A. Gervasi, *Corros. Sci.*, 51 (2009) 876.
25. C.S. Wu, Z. Zhang, F.H. Cao, L.J. Zhang, C.N. Cao, *Appl. Surf. Sci*., 253 (2007) 3893.
26. G. Grundmeier, W. Schmidt, and M. Stratmann, *Electrochim. Acta*, 45 (2000) 2515.
27. M. H. Abdullah, S. H. Ahmad, S. F. Jusoh, A. A. Mansor, and S. A. A. Hamid, *J. Appl. Phys*., 92 (2002) 876.
28. M. Laleh, A.S. Rouhaghdam, T. Shahrabi, A. Shanghi, *J. Alloys Compd*., 496 (2010) 548.
29. C. S. Wu, Z. Zhang, F. H. Cao, L. J. Zhang, and C. N. Cao, *Appl. Surf. Sci.*, 253 (2007) 3893.
30. Z. Shi, G. Song, and A. Atrens, *Corros. Sci.*, 47 (2005) 2760.
31. L. Chai, X. Yu, Z. Yang, Y. Wang, M. Okido, *Corros. Sci*., 50 (2008) 3274.
32. A. Valor, F. Caleyo, L. Alfonso, D. Rivas, J. Hallen, *Corros. Sci*., 49 (2007) 559.
33. M. A. Hernández, S. Valdez, *ECS. Trans.*, 36 (1) (2011) 55.
34. S. J. Xia, R. Yue, R. G. Rateick, V. I. Birss, *J. Electrochem. Soc*., 151 (2004) B179.
35. C. F. Zhu, R. Xie, J. H. Xue, L. L. Song, *Electrochim. Acta*, 56 (2011) 5828.
36. J. Liang, L. Hu, and J. Hao, *Electrochim. Acta*, 52 (2007) 4836.

37. M. L. Zheludkevich, K. A. Yasakau, A. C. Bastos, O. V. Karavai, M. G. S. Ferreira., *Electrochem. Commun*., 9 (2007) 2622.
38. J. G. He, J.B. Wen, X.D. Li, G.W. Wang, C.H. Xu, *Trans. Nonferr. Metal. Soc*., 21 (2011) 1580.
39. M. G. Pujar, T. Anita, H. Shaikh, R.K. Dayal, H. Khatak, *J. Mater. Eng. Perform.*, 16 (2007) 494.
40. Bernabe Carcel, Jesus Sampedro, Ana Ruescas, Xavier Toneul, *Phys. Proc*., 12 (2011) 353.
41. R. C. Grela, B. F. C. Illanes, S. V. Rodríguez, *Ings.*, 14 (50) (2011) 56.